35th Annual International Conference of the IEEE EMBS
Osaka, Japan, 3 - 7 July, 2013

Dual-band Multi-aperture Enhanced Redox Imaging of Colonic Adenomas for Endoscopes with a High-performance CMOS Imager

K. Kagawa, *Member, IEEE*, B. Zhang, M.-W. Seo, *Member, IEEE*, S. Kawahito, *Member, IEEE*, Y. Kominami, K. Yamada, S. Yoshida, S. Tanaka

Abstract— **Dual-band multi-aperture imaging of colonic adenomas based on the redox condition of mucosal cells for next-generation endoscopes is proposed. A low-noise and high-dynamic-range CMOS imager with the folding integration and the cyclic ADC is utilized in the single-imager multi-aperture camera system with 475-nm and 530-nm band-pass filters. A redox image is calculated from four kinds of images, 475-nm and 530-nm fluorescence images for 365-nm and 405-nm excitation lights. Dark current and random noise are reduced with a selective averaging method. The contrast of the redox image has been successfully enhanced.**

I. Introduction

To depict tumorous parts in the endoscopic observation, autofluorescence from metabolism-related fluorophores such as nicotinamide adenine dinucleotide (NADH) and flavin adenine dinucleotide (FAD) have been investigated [1](Fig. 1). To alleviate the effect of hemoglobin absorption, dual-wavelength excitation has been proposed [2]. In Ref. 2, two autofluorescence images for 450 to 490nm wavelengths, where HbO_2 shows local minimum in absorption, are serially taken for the excitation lights of two different wavelengths: 365nm and 405nm. The redox image is given by the ratio of the autofluorescence images for 365nm and 405nm excitation lights, that is, $F_{EX365,BP475}/ F_{EX405,BP475}$.

State-of-the-art CMOS imagers are very useful for observing autofluorescence images. Pixels with an in-pixel charge transfer structure, known as 4-transistor pixel based on a pinned photodiode [3], have significantly improved the image quality of CMOS imagers. In addition, thanks to integration of analog and digital processing circuits and column-parallel analog to digital converters, the performance of CMOS imagers on noise and dynamic range has overcome not only those of ordinary CCD imagers but high-sensitivity EM-CCD imagers. In general, the amplifier noise can be reduced as the amplifier gain increases. Instead, the dynamic range as well as the maximal signal level is reduced. We have achieved low noise, high sensitivity, and high dynamic range at the same time by the folding integration and the cyclic ADC. The noise level and the dynamic range have reached about one electron and 85dB, respectively [4].

It is known that most endoscopes have slow optics to obtain deep field of view. Due to hemoglobin absorption and lower absorption of fluorophores, autofluorescence images for 405-nm excitation are darker than those for 365-nm excitation. Therefore, low noise and high sensitivity are required for the imager. In addition, high dynamic range is necessary for observing objects with non-uniform hemoglobin concentration or outshoots, for which the intensity of effective excitation light spatially varies in a wide range depending on the lighting and hemoglobin absorption.

In this paper, a dual-band multi-aperture camera for enhanced redox imaging of colonic adenomas based on the low-noise high-sensitivity high-dynamic-range CMOS imager is proposed. In our previous works, functional multi-aperture endoscopes have been proposed, which include the features of stereoscopic endoscopes [5,6] and also offer several additional advantages. Multi-lens design allows to acquire multispectral images [7], polarization [8] for controlling the observable depth, and variable field-of-view [9].

530-nm fluorescence as well as 475-nm fluorescence is utilized in the proposed method to enhance the redox image. The redox image is calculated from four images: 475-nm and 530-nm fluorescence images for 365-nm and 405-nm excitation lights, namely, $F_{EX365,BP475}$, $F_{EX365,BP530}$, $F_{EX405,BP475}$, and $F_{EX405,BP530}$. Because 530 nm is the peak of the FAD fluorescence, multiplication of the two ratio images,

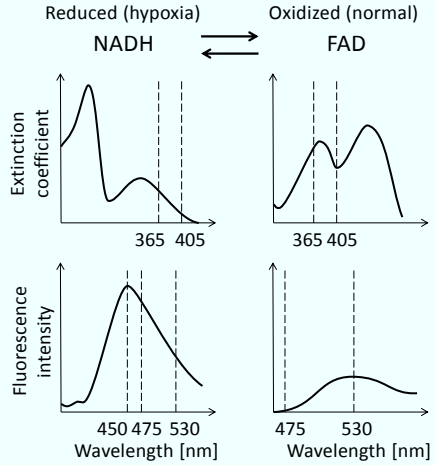

Fig. 1. Redox-related autofluorescence from biomaterials.

*Research supported by the Cooperative Research Project of Research Institute of Electronics, Shizuoka University.

K. Kagawa, B. Zhang, M.-W. Seo and S. Kawahito are with Research Institute of Electronics, Shizuoka University, 3-5-1 Johoku, Naka-ku, Hamamatsu, Shizuoka 432-8011, Japan (corresponding author to provide e-mail: kagawa@idl.rie.shizuoka.ac.jp).

K. Yamada is with Osaka University, 1-5 Yamadaoka, Suita, Osaka 565-0871, Japan.

Y. Kominami and S. Yoshida are with Hiroshima University Hospital, 1-2-3 Kasumi, Minami-ku, Hiroshima, Hiroshima 734-8551, Japan.

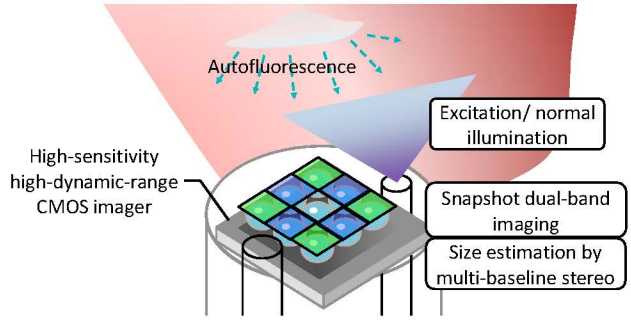

Fig. 2. The proposed autofluorescence endoscope

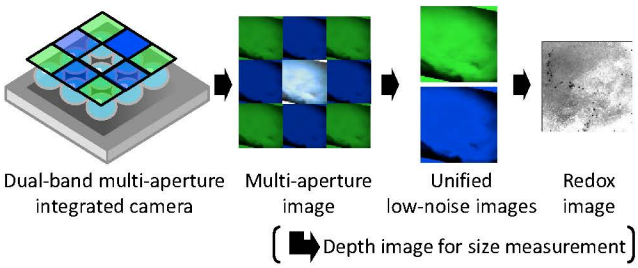

Fig. 3. Procedure of redox image reproduction.

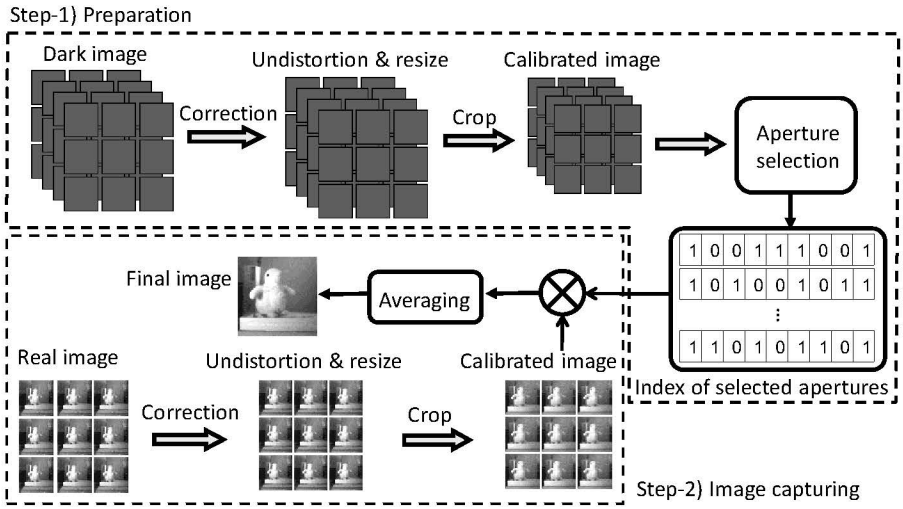

Fig. 4. Noise reduction scheme by selective averaging.

$F_{EX365,BP475}/F_{EX405,BP475}$ and $F_{EX365,BP530}/F_{EX405,BP530}$, is expected to increase the contrast of the redox image.

In the observation of weak fluorescence, dark current noise and pixel random noise become visible. Especially random telegraph (RTS) noise has become a significant issue in the state-of-the-art CMOS imagers [10]. The amount of these kinds of noise varies pixel by pixel. Although the number of pixels with outstanding noise is small, they are recognized as white defects or blinking pixels. To remove these kinds of noise, we have demonstrated that a selective averaging method with the multi-aperture camera can effectively reduce the dark current and the RTS noise at the same time. This method is also applied to reproduction of fluorescence images to further reduce the imager noise.

II. MULTIAPERTURE AUTOFLUORESCENCE IMAGING

A. Dual-band multi-aperture integrated camera

The configuration of the proposed dual-band multi-aperture integrated camera is shown in Fig. 2. The camera is composed of a single CMOS imager and 3×3 lenses. 475-nm band-pass filters are attached to four lenses, and 530-nm band-pass filters for other four lenses. No filter is attached to the centered lens to capture normal images. This configuration enables a snap-shot dual-band image acquisition for one excitation wavelength. Through the glass fiber, excitation or white light is conducted for illumination. This configuration is based on the thin observation module by bound optics (TOMBO) [11]. A drawback of the compound-eye approach is that the number of pixels for each lens is reduced compared with a conventional single-lens camera. The more images are captured for a wavelength, the better less noise becomes. However, there is a trade-off between the pixel count of the elemental image and the resultant image quality. We have selected 3×3 lenses.

B. Redox imaging by autofluorescence

Due to hypoxia, NADH increases in tumor cells. On the other hand, there is more oxygen in normal cells, so that FAD increases as suggested by Imaizumi,. As shown in Fig. 1, these biological fluorophores are excited by ultraviolet and deep blue lights. A redox image based on metabolism is given by $F_{EX365,BP475}/F_{EX405,BP475}$ with eliminating the effect of hemoglobin absorption.

In this paper, 530-nm fluorescence that corresponds to the peak wavelength of FAD is also used to enhance the contrast of the redox image. Here, redox image is defined by a product of two REDOX images for 475 nm and 530 nm to enhance the contrast as follows:

$$\mathrm{REDOX} = \frac{F_{EX365,BP475}}{F_{EX405,BP475}} \cdot \frac{F_{EX365,BP530}}{F_{EX405,BP530}}. \quad (1)$$

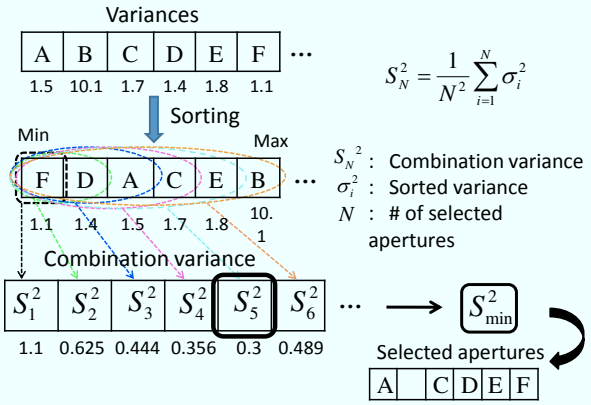

Fig. 5. Noise reduction scheme by selective averaging.

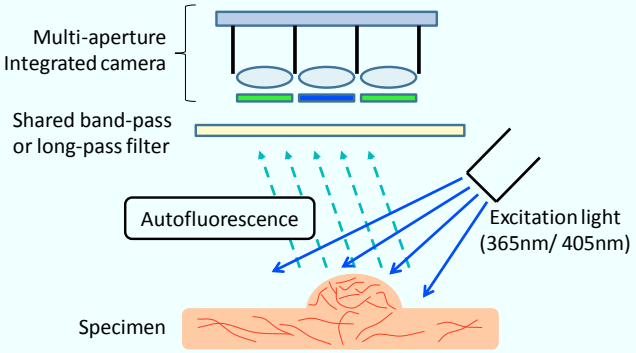

Fig. 6. Experimental setup.

Table I. Specifications of the CMOS imager.

Technology	0.18μm 1P4M CIS process
Pixel pitch [μm]	7.1 × 7.1
Fill factor [%]	45
Pixel count	1284 × 1028
Sensitivity [V/lx·s]	20@3746K with IR cut
ADC resolution [b]	17
Dynamic range [dB]	85.0
Frame rate [fps]	30

Table II. Specifications of the multi-aperture camera.

Focal length [mm]	3.0
F-number	3.0
Full field of view [degree]	27
Number of lenses	3 × 3
Lens pitch [mm]	2.1
Pixel count per lens	200 × 200

Fig. 3 shows the flow chart to calculate redox images. The images for the same band-pass filter are unified as mentioned below. Then, REDOX is calculated based on Eq. 1.

III. Noise Reduction by Selective Averaging[12]

An M-aperture system shown in Fig. 4 (M=3×3) is considered, which means that M images are obtained at the same time for the same object. However, the pixel values for an identical objective point are not exactly the same, because different random noise and dark current noise are added to every pixel. In the preparation step, the camera parameters are extracted, and dark images are captured to measure the variance of every pixel and aperture. Fig. 5 shows a flow for calculating the variance for one pixel from multiple apertures. The variances are sorted from the minimum to the maximum. Then, a combination variance is calculated by using the following equation:

$$S_N^2 = \frac{1}{N^2}\sum_{i=1}^{N}\sigma_i^2. \qquad (1 \le N \le M) \qquad (2)$$

Here, N is the number of selected apertures, σ^2 is the sorted variance, and S_N^2 is the combination variance. From the calculated combination variance, we can find out the minimum one and the index of combined apertures. For nominal noise, S_N^2 decreases as N increases. However, for large σ_N^2, S_N^2 can be bigger than S_{N-1}^2. When it is the case, the apertures $\{i\}$ $(i \ge N)$ are not selected. Thus, large RTS noise and large dark current that causes large shot noise can be removed.

IV. Experimental Results

A. System configuration

The setup of an experimental system is shown in Fig. 6. The specifications of the CMOS imager and a prototype multi-aperture camera are summarized in Tables I and II. As excitation light sources, a UV LED light (KENKO-TOKINA, UVLED illuminator, spot type, 365 nm) and a deep-blue LED light (KENKO-TOKINA, UVLED illuminator, spot type, 405nm) were used. Acrylic band-pass filters for 475 nm (Fujifilm, BPB-45) and 530 nm (Fujifilm, BPB-53) were attached to the multi-aperture camera with a shared long-pass filter (Edmund Optics, High performance OD4 long-pass filter, 450nm). A band-pass filter for 475 nm (Edmund Optics, Fluorescence band-pass filter, 475 nm×50 nm) was used to reproduce a reference image by the conventional method. In this case, images for the centered lens, that has no filter, were used. The frame rate of the CMOS imager was 15 fps, namely, exposure time was 66 ms.

B. Autofluorescence images and noise reduction

Fig. 7 shows an example of endoscopic picture of colonic adenoma of human, which was captured by a conventional endoscope. Fig. 8 shows *ex-vivo* multi-aperture fluorescence images for two excitation wavelengths, which correspond to Fig. 7. The study has been applied for full approval of the ethics committee of Hiroshima University. On the observed plane, the optical powers for 365-nm and 405-nm excitation lights were 7.4 mW/cm^2 and 7.2 mW/cm^2, respectively. Fig. 9 compared one out of four apertures for the 405-nm excitation and 475-nm fluorescence and the result of noise reduction by the selective averaging. In Fig. 10(a), there are

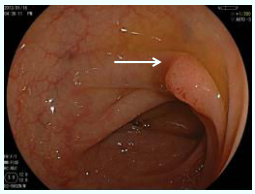

Fig. 7. An endoscopic image of tubular adenoma of colon.

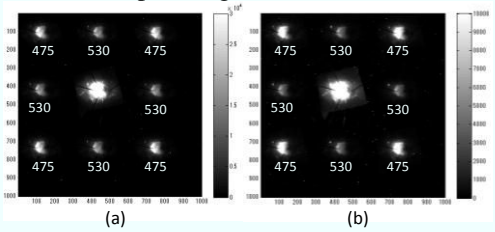

Fig. 8. Example *ex-vivo* multi-aperture images for excitation light of (a) 365 nm and (b) 405 nm.

white spots caused by large dark current and RTS noise. In contrast, they were completely removed by the selective averaging, and the signal-to-noise ratio was improved because of averaging.

C. Redox imaging

Fig. 11 compares redox images by Imaizumi's method and the proposed method. An NADH-rich part becomes brighter than the other normal part. An end of lesioned part is indicated by arrow. It is shown that the contrast of the lesioned part is enhanced by the proposed method. Fig. 12 shows an endoscopic picture and redox images for another colonic adenoma. It is confirmed that the contrast for the proposed method is also enhanced. These images were compared to histopathological results.

V. Conclusion

Dual-band multi-aperture imaging of colonic adenomas based on mucosal redox condition has been proposed. Based on a low-noise high-sensitivity high-dynamic-range CMOS imager and the selective averaging method, less noisy fluorescence images have been reproduced. Redox images were calculated from four kinds of images, 475-nm and 530-nm fluorescence images for 365-nm and 405-nm excitation lights. The contrast in the redox image has been successfully enhanced.

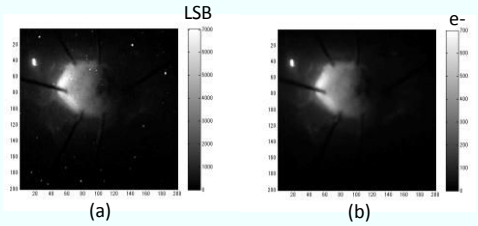

Fig. 9. Noise reduction results for excitation of 405 nm and fluorescence of 530 nm: (a) original one aperture and (b) selective averaging from four apertures.

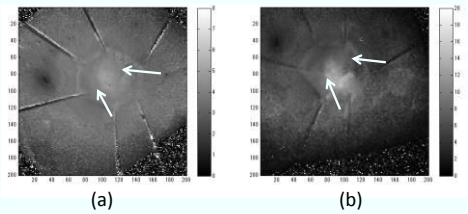

Fig. 10. Redox images: (a) conventional and (b) proposed.

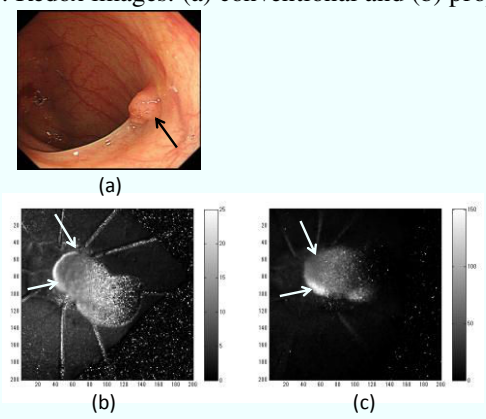

Fig. 11. Redox image of another tubular adenoma: (a) endoscopic picture, (b) conventional and (c) proposed.

References

[1] N. Kirkpatrick, C. Zou, M. Brewer, W. Brands, R. Drezek, and U. Utzinger, "Endogenous fluorescence spectroscopy of cell suspensions for chemopreventive drug monisotring," Photochemistry and Photobiology **81**, pp. 125-134 (2005).

[2] K. Imaizumi, Y. Harada, N. Wakabayashi, Y. Yamaoka, H. Konishi, P. Dai, H. Tanaka, and T. Takamatsu, "Dual-wavelength excitation of mucosal autofluorescence for precise detection of diminutive colonic adenomas," Gastrointestinal Endoscopy **75**, pp. 110-117 (2012).

[3] 12. P. Lee, R. Gee, R. Guidash, T-H. Lee, and E. Fossum, "An active pixel sensor fabricated using CMOS/CCD process technology," Proc. 1995 IEEE Workshop on CCDs and AISs (1995).

[4] M. Seo, T. Sawamoto, T. Akahori, Z. Liu, T. Iida, T. Takasawa, T. Kosugi, T. Watanabe, K. Isobe, and S. Kawahito, "A low-noise high-dynamic-range 17-b 1.3-Megapixel 30-fps CMOS image sensor with column-parallel two-stage folding-integration/cyclic ADC," IEEE Trans. Electron Dev. **59**, pp. 3396-3400 (2012).

[5] K. Yamada, H. Mitsui, and K. Kishimoto, "Small capturing system of three-dimensional image using compound optics," Int. J. Innovative Computing, Information and Control **5**, 735-741 (2009).

[6] K. Kagawa, K. Yamada, E. Tanaka, and J. Tanida, "Three-dimensional multi-functional compound-eye endoscopic system with extended depth of field, " IEEJ Trans. Electronics, Information and Systems 32, pp. 120-130 (2012).

[7] J. Tanida, R. Shogenji, Y. Kitamura, K. Yamada, M. Miyamoto, and S. Miyatake, "Color imaging with an integrated compound imaging system," Opt. Exp. **11**, 2109-2117 (2003).

[8] K. Kagawa, E. Tanaka, K. Yamada, S. Kawahito, and J. Tanida, "Deep-focus compound-eye camera with polarization filters for 3D endoscopes, " in Proc. of 2012 Photonics West, 8227-42 (2012).

[9] K. Kagawa, R. Shogenji, E. Tanaka, K. Yamada, S. Kawahito, and J. Tanida, "Variable field-of-view visible and near-infrared polarization compound-eye endoscope," in Proc. of Int'l Conf. of Engineering in Medicine and Biology Society (EMBC2012), pp. 3720-3723 (2012).

[10] P. Gonthier and P. Magnan, "RTS noise impact in CMOS image sensors readout circuits," in Proc. of 16th IEEE Int'l. Conf. on Electronics, Circuits and Systems (ICECS), pp. 928-031 (2010).

[11] J. Tanida, T. Kumagai, K. Yamada, S. Miyatake, K. Ishida, T. Morimoto, N. Kondou, D. Miyazaki, and Y. Ichioka, "Thin observation module by bound optics (TOMBO), concept and experimental verification," Appl. Opt. **40**, 1806-1819 (2001).

[12] B. Zhang, K. Kagawa, M. Seo, K. Yasutomi, and S. Kawahito, "RTS noise and dark current reduction using selevtive averaging with multi-aperture system," in Proc. of ITE Annual Convention, 17-1 (2011).